Mechanistic and Spatial Study of Ultrasonically Induced Luminol Chemiluminescence

ARTICLE *in* THE JOURNAL OF PHYSICAL CHEMISTRY A · MAY 1999

Impact Factor: 2.69 · DOI: 10.1021/jp984503r

2 AUTHORS, INCLUDING:

Benjamin Paul Wilson
Aalto University
25 PUBLICATIONS **189** CITATIONS

SEE PROFILE

Mechanistic and Spatial Study of Ultrasonically Induced Luminol Chemiluminescence

H. N. McMurray* and B. P. Wilson

Department of Materials Engineering, University of Wales Swansea, Singleton Park, Swansea, SA2 8PP, U.K.

Received: November 23, 1998; In Final Form: February 16, 1999

Aqueous solutions containing 10^{-3} M luminol and varying concentrations of hydrogen peroxide are irradiated with 20 kHz ultrasound at 50 °C. The intensity of sonogenerated chemiluminescence (SCL) is shown to increase linearly with ultrasound power and to be strongly pH dependent, reaching a maximum at pH 12. For pH < 10 SCL intensity (I_{SCL}) is independent of H_2O_2 concentration. For pH >10 I_{SCL} increases monotonically with H_2O_2 concentration up to10^{-4} M but decreases as the concentration is increased further. A mechanism is proposed in which HO_2^- and the luminol monoanion competitively reduce sonochemically generated $HO^\bullet$, producing $O_2^{\bullet-}$ and luminol radical anion, respectively. Luminescence follows the decomposition of a hydroperoxide adduct formed by reaction between $O_2^{\bullet-}$ and luminol radical anion. EDTA is shown to suppress the background (silent) chemiluminescence of solutions containing luminol and H_2O_2 without significantly affecting I_{SCL}. Digital images of SCL emission occurring near the transducer−solution interface are analyzed to determine the spatial distribution of sonochemical activity. It is shown that, in the absence of standing waves, I_{SCL} decays exponentially with perpendicular distance from the surface of a plane-ended ultrasound transducer horn. Spatially resolved I_{SCL} data is used to determine the acoustic attenuation coefficient (α) in acoustically cavitating water noninvasively. It is shown that α values at the cavitation-producing frequency increase with transducer output power and may be many orders of magnitude greater than is the case for homogeneous water.

Introduction

It is well-known that alkaline solutions of luminol emit light when subject to ultrasound of sufficient intensity to produce acoustic cavitation. Light emission is believed to occur through a process of oxidative chemiluminescence involving sonochemically generated $HO^\bullet$ and is orders of magnitude more intense than the natural sonoluminescence of aerated water.[1−5] The sonogenerated chemiluminescence (SCL) of luminol has been used to study the mechanics of cavitation.[1,3] It has also been used to visualize the spatial distribution of cavitation in solution, either photographically[4,5] or using a scanned fiber-optic probe.[5] However, relatively little is known regarding the kinetics and mechanism of luminol SCL.

Previous mechanistic studies of luminol chemiluminescence[6,7] and electrogenerated chemiluminescence (ECL)[8,9] in aqueous solution have shown that the intensity of light emission is strongly influenced by solution pH and by the concentration of hydrogen peroxide. It has been our aim to determine the extent to which similar relationships exist in the case of luminol SCL and to exploit these in elucidating the SCL mechanism. It has been our further aim to use digital images of the luminescent volume of solution near the ultrasound transducer−solution interface to obtain spatially resolved SCL intensity data. This was done in order to investigate the absorption of ultrasound energy propagating within the bubble field generated through acoustic cavitation by determining the distribution of sonochemical activity so produced.

All the work to be described was carried out in air-equilibrated water, as this is the medium in which a majority of the current technological applications of power ultrasound occur. Furthermore, to maximize cavitation and hence the absorption of ultrasound by cavitation bubbles a slightly elevated temperature (50 °C) has been used throughout.[10] Sonochemical yields in aqueous systems tend to decrease with increasing temperature,[11] but luminol SCL intensities are sufficient for quantitative studies at 50 °C.

The study of luminol SCL in the presence of H_2O_2 is potentially complicated by a background (nonsonochemical) process of chemiluminescence catalyzed by trace concentrations of divalent transition metal cations.[12−15] Transition metal contamination of solutions through impurities present in reagents or through leaching from equipment is difficult to avoid completely. However, chelating agents such as EDTA are known to complex the cations involved, greatly reducing their catalytic activity.[12,13] Here we show how EDTA may be used to suppress the background chemiluminescence of aqueous solutions containing luminol and H_2O_2 while minimally affecting SCL, thus simplifying the acquisition of SCL intensity data.

Experimental Section

Materials. Luminol (3-aminophthalhydrazide, 97%) and hydrogen peroxide (unstabilized, aqueous 30% w/w) were obtained from the Aldrich Chemical Co. Ltd. All other reagents were obtained at Analar grade purity from Fischer Chemicals Ltd. All reagents were used without further purification. Doubly distilled water was used throughout for the preparation of solutions. All luminol solutions for SCL experiments contained 0.1 M Na_2HPO_4 as a pH buffer, and solution pH was adjusted using equinormal solutions of NaOH or H_3PO_4. Concentrations of EDTA in luminol solutions for SCL were established using volumetric additions of 0.02 M aqueous tetrasodium EDTA. Concentrations of H_2O_2 in luminol solutions for SCL were established using volumetric additions of 0.02 M aqueous H_2O_2 prepared by volumetric dilution of the 30% stock. All solutions containing dilute H_2O_2 were used within 12 h of preparation.

10.1021/jp984503r CCC: $18.00
Published on Web 05/04/1999

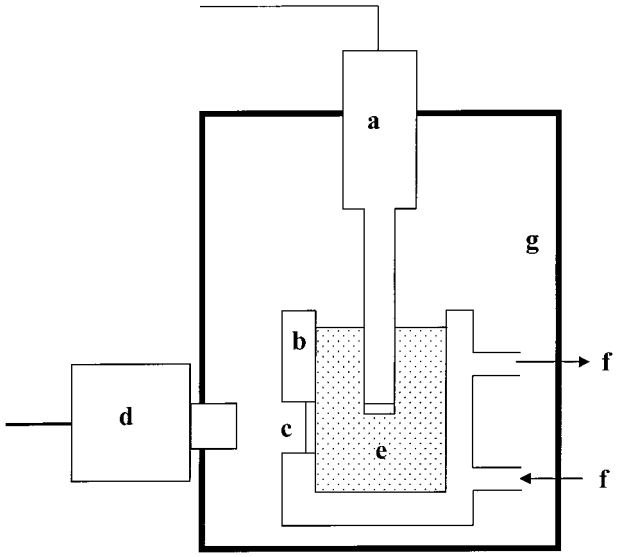

Figure 1. Schematic diagram of experimental apparatus: (a) ultrasound generator; (b) thermostated cell; (c) optically flat window; (d) photomultiplier tube or video camera; (e) solution containing luminol; (f) thermostated water from circulator; (g) light-proof box.

Methods. The apparatus used for SCL and chemiluminescent light intensity measurements and for SCL image acquisition is shown schematically in Figure 1. The ultrasound source was a 20 kHz Branson Sonifier 250 variable power ultrasound generator and piezoelectric transducer horn. The transducer horn was used in conjunction with 1 cm diameter cylindrical titanium sonoprobe tips. All spatially unresolved SCL measurements were performed using a plane-ended tip. Spatially resolved (imaging) experiments were performed using both the plane-ended tip and a similar tip terminated in a "wedge" section with a vertex angle of 45°. Ultrasound output power was calibrated using a calorimetric method.[16] All SCL experiments were carried out in a glass cell fitted with an optically flat window and a water jacket through which water was circulated from a Grant Y14 thermostated water bath. In all cases, the volume of the sonicated solution was approximately 100 cm^3 and this solution was in contact with room air. The distances between the sonoprobe tip, the cell walls, and the solution air interface were such that a standing wave pattern did not become established.

Spatially unresolved light intensity measurements were performed using a type QL30F photomultiplier tube and type A1 transconductance amplifier supplied by Electron Tubes Ltd. Light from the luminescent volume of solution was focused onto the photocathode using a 3 cm diameter compound glass lens of 10 cm focal length. SCL imaging and spatially resolved light intensity measurements were performed using a Merlin LIC-216-F40E image intensified CCD video camera and type CCU 2025 camera control unit supplied by Custom Cameras Ltd. The camera was fitted with a Zeiss 55 mm f2 lens. Monochrome images of 320 × 240 pixels were digitized with 8 bit grayscale resolution using a video capture card and software supplied by Motion Picture Ltd. Images were captured from single video frames, or integrated over 64 frames for improved signal-to-noise ratio. Image analysis and isoluminance contour plot generation was performed using "Surfer" cartography software obtained from Golden Software Ltd. In all cases where digitized images were subject to quantitative analysis care was taken that the image bitmap contained no areas of saturation, i.e., that all the 8 bit pixel values fell between 0 and 255. Care was also taken that the camera's depth of field was adequate to keep the luminescent feature in sharp focus. The object distance was typically 40 cm.

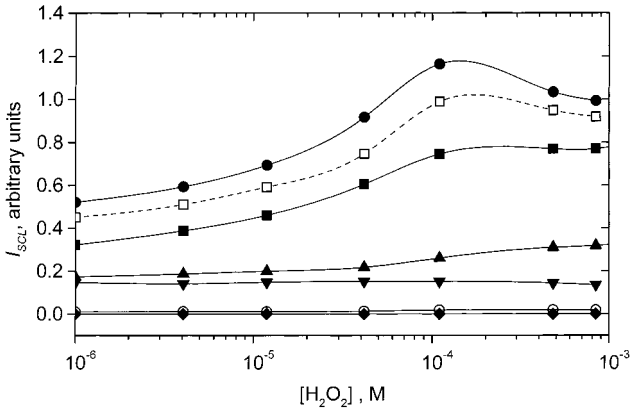

Figure 2. The effect of H_2O_2 concentration on spatially unresolved I_{SCL} at different values of solution pH; luminol concentration = 10^{-3} M; EDTA = concentration 10^{-4} M; temperature = 50 °C; ultrasound power = 70 W; (◆) pH 7; (○) pH 8; (▼) pH 9; (▲) pH 10; (■) pH 11; (●) pH 12; (□) pH 13.

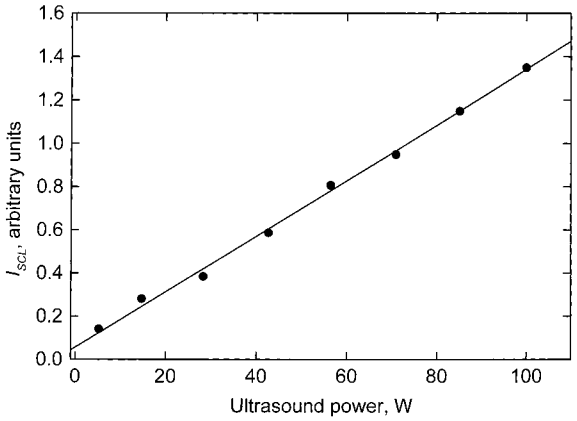

Figure 3. Relationship between ultrasound output power and spatially unresolved I_{SCL}: luminol concentration = 10^{-3} M; H_2O_2 concentration = 10^{-4} M; EDTA concentration = 10^{-4} M; temperature = 50 °C; pH = 12.

Results and Discussion

Effect of H_2O_2 Concentration, EDTA Concentration, and pH. The influence of H_2O_2 concentration ($[H_2O_2]$) on spatially unresolved SCL intensity was studied over a range of solution pH at constant temperature and using constant ultrasound power. Figure 2 shows the relative intensity of SCL emission (I_{SCL}) as a function of $[H_2O_2]$ obtained from a solution containing luminol and EDTA at pH values between pH 7 and pH 13. It may be seen from Figure 2 that at any given value of $[H_2O_2]$ I_{SCL} increases monotonically with solution pH up to pH 12. Above pH 12, the trend becomes reversed and I_{SCL} is decreased at pH 13. It may also be seen from Figure 2 that at pH ≤ 10 increasing $[H_2O_2]$ has no significant effect on I_{SCL}. However, at pH > 10 I_{SCL} increases monotonically with increasing $[H_2O_2]$ for $[H_2O_2]$ < 10^{-4} M. This effect is greatest at pH 12, where the value of I_{SCL} approximately doubles as $[H_2O_2]$ increases from 10^{-6} M to = 10^{-4} M. At $[H_2O_2]$ > 10^{-4} M the trend is reversed and I_{SCL} decreases with increasing H_2O_2 concentration. The dependence of I_{SCL} on ultrasound power was investigated at pH 12 using a solution containing luminol, EDTA, and 10^{-4} M H_2O_2. Figure 3 shows the substantially linear (linear correlation coefficient 0.9998) relationship observed between I_{SCL} and ultrasonic output power under these conditions. The observed dependencies of I_{SCL} on pH, $[H_2O_2]$, and ultrasound power will be discussed in terms of the SCL mechanism in subsequent sections.

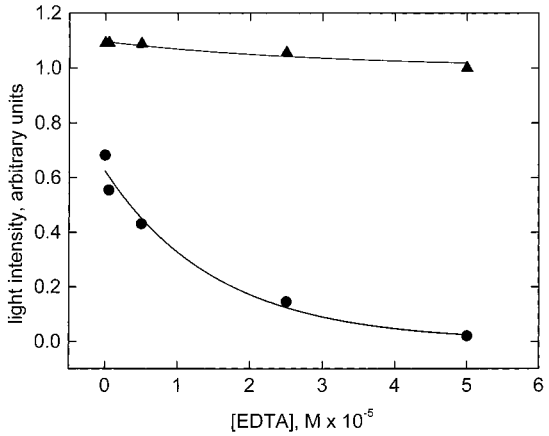

Figure 4. Effect of EDTA concentration on spatially unresolved intensity of luminol chemiluminescence under (▲) sonicated and (●) silent conditions: luminol concentration = 10^{-3} M; H_2O_2 concentration = 10^{-4} M; temperature = 50 °C; solution pH = 12; ultrasound power = 70 W.

The effect of EDTA in suppressing the background (silent) chemiluminescence of aqueous luminol/H_2O_2 is illustrated in Figure 4. Figure 4 shows the relative intensity of light emitted by a solution containing luminol and H_2O_2 at pH 12 as a function of EDTA concentration, under both sonicated and silent conditions. It may be seen from Figure 4 that the addition of EDTA has little effect on I_{SCL}, which decreases by <5% as the EDTA concentration increases from 0 to 5×10^{-5} M. However, it may also be seen from Figure 4 that the intensity of chemiluminescence under silent conditions decreases monotonically with increasing EDTA concentration and is reduced by approximately 95% at an EDTA concentration of 5×10^{-5} M.

Aqueous solutions of divalent transition metal cations such as Cu^{2+}, Fe^{2+}, Co^{2+}, and Mn^{2+} are well known to catalyze the chemiluminescence of luminol in the presence of dissolved O_2 and/or H_2O_2.[12−14] In the presence of H_2O_2, significant increases in emitted light intensity may be produced by even trace concentrations of transition metal cations.[14] The exact mechanism of this transition metal catalysis is not known but the production of $HO^\bullet$ through a Fenton type reaction has been suggest as an important step,[12] i.e.,

$$M^{2+} + H_2O_2 \rightarrow M^{3+} + HO^- + HO^\bullet \quad (1)$$

It is also known that the complexation of divalent transition metal cations by chelating agents such as EDTA greatly diminishes their ability to catalyze luminol chemiluminescence.[12,14] On the basis of the above it is first proposed that the levels of background light emission observed in the absence of added EDTA result from luminol chemiluminescence catalyzed by traces of transition metal cation present in the reagents and/or water used in our experiments. Metal cations leaching from apparatus and glassware could also contribute. It is further proposed that the observed suppression of background chemiluminescence by EDTA results from the complexation and deactivation of trace transition metal cations. The finding that I_{SCL} is not significantly reduced at EDTA concentrations up to 5×10^{-5} M implies that EDTA acts specifically to inhibit the background chemiluminescence. This suggests that EDTA cannot be acting as a reductive "quencher" for $HO^\bullet$ or $O_2^{\bullet-}$ radials (vidi infra) and so tends to confirm the hypothesis that it is the properties of EDTA as a chelating agent which are important here.

The use of a pH buffer in experiments aimed at elucidating the kinetics and mechanism of luminol SCL must be regarded as a necessary evil. The various ionic forms of phosphate, and alternative buffer species such as borate and (bi-)carbonate, may react with radicals such as $HO^\bullet$ and therefore cannot be regarded as inert.[17−20] However, changing the concentration of phosphate buffer from 10^{-3} to 10^{-1} M at pH 11.0 in the presence of 5×10^{-5} M EDTA and varying concentrations of H_2O_2 was not found to produce any significant change in I_{SCL} values. For this reason, phosphate-derived species will not be considered in any subsequent discussion of the luminol SCL mechanism.

Sonochemical Generation of $HO^\bullet$ and $O_2^{\bullet-}$. The cyclic pressure variations associated with the propagation of ultrasound waves in aqueous solution are known to result in the nucleation, growth, and periodic collapse of microscopic cavitation bubbles filled with gas and/or vapor.[16,21] Furthermore, it has been shown that extremely high local temperatures and pressures may be generated during the collapse or implosion of such bubbles.[16,21] Consequently, it is generally accepted that it is within the cavitation bubble, or the layer of solution immediately contacting the cavitation bubble, that the sonochemical effects of molecular activation and dissociation take place.[16,21−23] In air-saturated water, the principal sonochemical dissociation processes involve the homolytic cleavage of H_2O and dissolved O_2.[24−26]

$$H_2O \rightarrow H^\bullet + HO^\bullet \quad (2)$$

$$O_2 \rightarrow O + O \quad (3)$$

The cleavage products may then recombine or react further as below:

$$HO^\bullet + HO^\bullet \rightarrow H_2O_2 \quad (4)$$

$$O + H_2O \rightarrow HO^\bullet + HO^\bullet \quad (5)$$

$$H^\bullet + O_2 \rightarrow HO_2^\bullet \quad (6)$$

$$HO_2^\bullet + HO_2^\bullet \rightarrow H_2O_2 + O_2 \quad (7)$$

Both hydroxyl radicals ($HO^\bullet$) and hydrogen atoms ($H^\bullet$) have been detected in ESR spin trapping experiments when water-containing permanent gases in solution is subject to ultrasound.[1,24,27] The production of hydroperoxyl radical ($HO_2^\bullet$) has been inferred from the involvement of this species in specific sonochemical reactions.[28−30] Furthermore, the sonochemical generation of H_2O_2 is well documented, and reactions 4−7 are reported to be significant routes of H_2O_2 formation.[1,31−33]

It should be noted that $HO_2^\bullet$ is a weak acid, $pK_a = 4.8$,[34] and at neutral and higher pH immediately dissociates to give the superoxide anion radical ($O_2^{\bullet-}$).

$$HO_2^\bullet \rightleftharpoons H^+ + O_2^{\bullet-} \quad (8)$$

H_2O_2 is also a weak acid, pK_a $10^{-11.65}$, and dissociates to give the hydroperoxyl anion (HO_2^-). The $HO^\bullet$ radical has a redox potential of 2.8 V[35] and is readily capable of oxidizing both H_2O_2 and HO_2^-. Thus, when significant concentrations of H_2O_2 are present in the sonicated solution, the following reactions will become important:

$$HO^\bullet + H_2O_2 \xrightarrow{k_9} O_2^{\bullet-} + H_3O^+ \quad (9)$$

$$HO^{\bullet} + HO_2^- \xrightarrow{k_{10}} O_2^{\bullet -} + H_2O \qquad (10)$$

The second-order rate constants k_9 and k_{10} have been determined to be 3.7×10^7 M^{-1} s^{-1} and $k_9 = 6.7 \times 10^9$ M^{-1} s^{-1} respectively.[7] Thus, the rate of $O_2^{\bullet -}$ production through reactions 9 and 10 is predicted to increase with pH as a result of the dissociation of H_2O_2.

Luminol SCL Mechanism. A number of mechanistic pathways have been proposed as contributing to the oxidative chemiluminescence of luminol and the interplay between these pathways is potentially complex.[6,7,36] Here we propose that the principal mechanism leading to luminol SCL under our experimental conditions is that shown in Scheme 1, which is similar to the mechanism proposed in the case of luminol chemiluminescence induced by γ-ray radiolysis.[6] Luminol is a weak dibasic acid with first and second pK_a values of 6.3[37] and ~13,[9] respectively. It may therefore be understood that over the experimental pH range the predominant luminol species will be the luminol monoanion (**I**). Step (i) in Scheme 1 is the oxidation of **I** by $HO^{\bullet}$ to produce the diazaquinone radical anion **II**. Step (ii) is the reaction of **II** with $O_2^{\bullet -}$ to form the hydroperoxide addition product **III**. **III** is a weak acid, pK_a = 10.4,[7] and it is only the monoanion form of **III**, which decomposes through step (iii) to give the exited state of the aminophthalate monoanion **IV**.[6,7] The neutral form of **III** decomposes via a dark reaction (iv) to give the starting material (**I**) and O_2. Step (iii) is thought to proceed via a concerted mechanism involving an unstable endoperoxide intermediate,[7] and the aminophthalate product **IV** relaxes to the ground state with emission of light at 430 nm.

If we consider SCL occurring in the absence of added H_2O_2, conditions approximated by the lowest H_2O_2 concentration data in Figure 2, $O_2^{\bullet -}$ will be produced directly through the dissociation of $HO_2^{\bullet}$ produced by reaction 6. Some H_2O_2 will be generated internally through reactions 4 and 7 and this may be oxidized to $O_2^{\bullet -}$ through reactions 9 and 10. In addition, $O_2^{\bullet -}$ is produced through the slow reaction of **II** with O_2 through reaction 11 below. Thus, sufficient $O_2^{\bullet -}$ will be present for light to be emitted through Scheme 1. The monotonic increase in I_{SCL} with pH seen in Figure 2 at pH $\leq$ 12 may be explained by the progressive dissociation of the hydroperoxide **III**.[7] The observed decrease in I_{SCL} at pH > 12 is consistent with the known decrease in quantum yield of aminophthalate luminescence at high pH.[7] The finding that increasing H_2O_2 concentration only increases I_{SCL} at pH $\geq$ 10 may be explained if we assume the rate of reaction 10 is fast enough to significantly increase the steady-state concentration of $O_2^{\bullet -}$, whereas the rate of reaction 9 is not.[6] This assumption would seem reasonable given the relative values of k_9 and k_{10}.

Regarding the I_{SCL} maxima observable in the pH 12 and pH 13 data shown in Figure 2, it may be understood that reaction 10 and step (i) of Scheme 1 are in direct competition for sonochemically generated $HO^{\bullet}$. Furthermore, it has been shown that this competition leads to maximum light emission occurring when the steady-state concentrations of **II** and $O_2^{\bullet -}$ are equal.[6] Thus, the observed reduction in I_{SCL} values at H_2O_2 concentrations of $>10^{-4}$ M may be ascribed to the depletion of $HO^{\bullet}$ through reaction 10 suppressing reaction step (i) and leading to a condition where the steady-state concentration of **II** is less than the concentration of $O_2^{\bullet -}$. The second-order rate constant for step (i) of Scheme 1 has been reported as 8.7×10^9 M^{-1} s^{-1},[38] i.e., similar to the value of k_{10} and close to the diffusion limit. This would suggest that at pH $\geq$ 12 maximum light emission should occur when the concentrations of luminol and hydrogen peroxide are approximately equal, provided **II** and $O_2^{\bullet -}$ are consumed at a similar rate. The finding that I_{SCL} is maximal at a luminol/H_2O_2 concentration ratio of ~10:1 suggests that **II** is actually consumed more rapidly than $O_2^{\bullet -}$. This would seem probable given the additional reactions in which **II** is known to be involved (vidi infra).

In addition to involvement in step (ii) of Scheme 1 ($k_{(ii)} \approx 10^{-7}$ M^{-1} s^{-1})[6] **II** has been shown to react slowly (forward rate constant $k_f(O_2 + \mathbf{II}) \approx 550$ M^{-1} s^{-1}) with molecular oxygen through the formal equilibrium

$$\mathbf{II} + O_2 \rightleftharpoons O_2^{\bullet -} + \text{diazaquinone} \qquad (11)$$

to give a neutral diazaquinone product.[7,36] **II** is also known to undergo rapid self-recombination and quantitative dismutation ($k_{12} = 5 \times 10^8$ M^{-1} s^{-1})[7,39] to give **I** and the same neutral diazaquinone.

$$\mathbf{II} + \mathbf{II} + H_2O \rightarrow \mathbf{I} + \text{diazaquinone} + HO^- \qquad (12)$$

The neutral diazaquinone product may either be destroyed through hydrolysis ($k(OH^- + \text{diazaquinone}) \approx 10^7$ M^{-1} s^{-1})[7] or react with HO_2^- to produce the hydroperoxide adduct **III** ($k(HO_2^- + \text{diazaquinone}) \approx 10^8$ M^{-1} s^{-1}).[7] The small value of k_f for reaction 11 implies that the formal equilibrium is never actually attained. In comparison with **II** $O_2^{\bullet -}$ is relatively stable with respect to dismutation to O_2 and H_2O_2 over the range of experimental pH used here.[40] Furthermore, the steady-state concentration of $O_2^{\bullet -}$ may be augmented through reaction 11 and the reaction of neutral diazaquinone with HO_2^-.

One consequence of the competition between reaction 10 and step (i) of Scheme 1 is that I_{SCL} is primarily determined by the ratio of luminol and H_2O_2 concentrations.[6] The absolute concentrations of luminol and H_2O_2 are immaterial, provided they are greater that the steady-state concentration of $HO^{\bullet}$.[6] Under conditions of alkaline pH and constant H_2O_2/luminol concentration ratio it has been shown that the integrated intensity of light emission is linearly dependent on γ-ray pulse radiolytic dose and hence $HO^{\bullet}$ yield.[6] Thus, the linear dependence of I_{SCL} on ultrasound output power shown in Figure 3 is consistent with the rate of sonochemical $HO^{\bullet}$ generation being directly proportional to the ultrasound power entering solution. It should be noted that nonlinear and even inverse relationships have been reported between I_{SCL} and ultrasound power at high transducer power levels.[2,4] However, we have not observed such relationships under our experimental conditions.

SCL Imaging. All SCL image acquisition experiments were carried out in solutions containing 10^{-3} M luminol, 10^{-4} M H_2O_2, and 10^{-4} M EDTA at pH 12. Parts a and b of Figure 5 show images of SCL activity in the region of a plane-ended and wedge-ended 1 cm diameter cylindrical titanium sonoprobe tip, respectively. These images were each obtained by the integration of 64 video frames, captured at 25 frame s^{-1}. In both parts a and b of Figure 5 a primary lobe or "plume" of luminescence can be seen extending into the solution such that the luminescent plume is coaxial with the ultrasound transducer horn. In the case of the wedge ended sonoprobe tip, Figure 5b shows secondary lobes of luminescence at the base angles of the wedge section where it joins the main body of the tip. The localization of SCL activity in Figure 5a is similar to that reported previously in the case of a plane ended 20 kHz transducer horn.[1] Furthermore, the SCL images obtained using the planar sonoprobe tip were uninfluenced by the volume of the sonicated solution or the dimensions of the sonication cell,

SCHEME 1. Reaction Pathways of Luminol Sonogenerated Chemiluminescence (SCL)

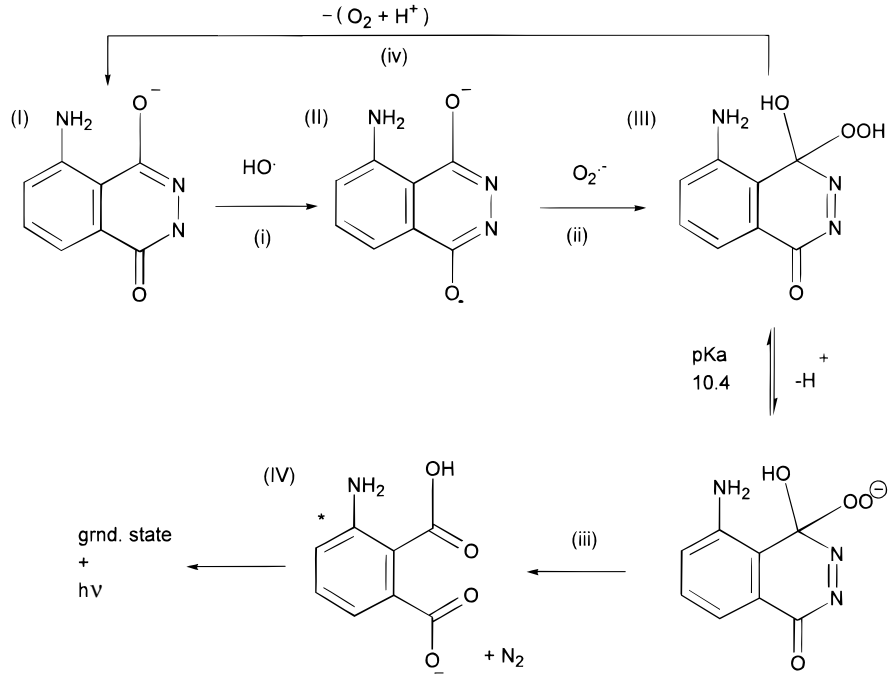

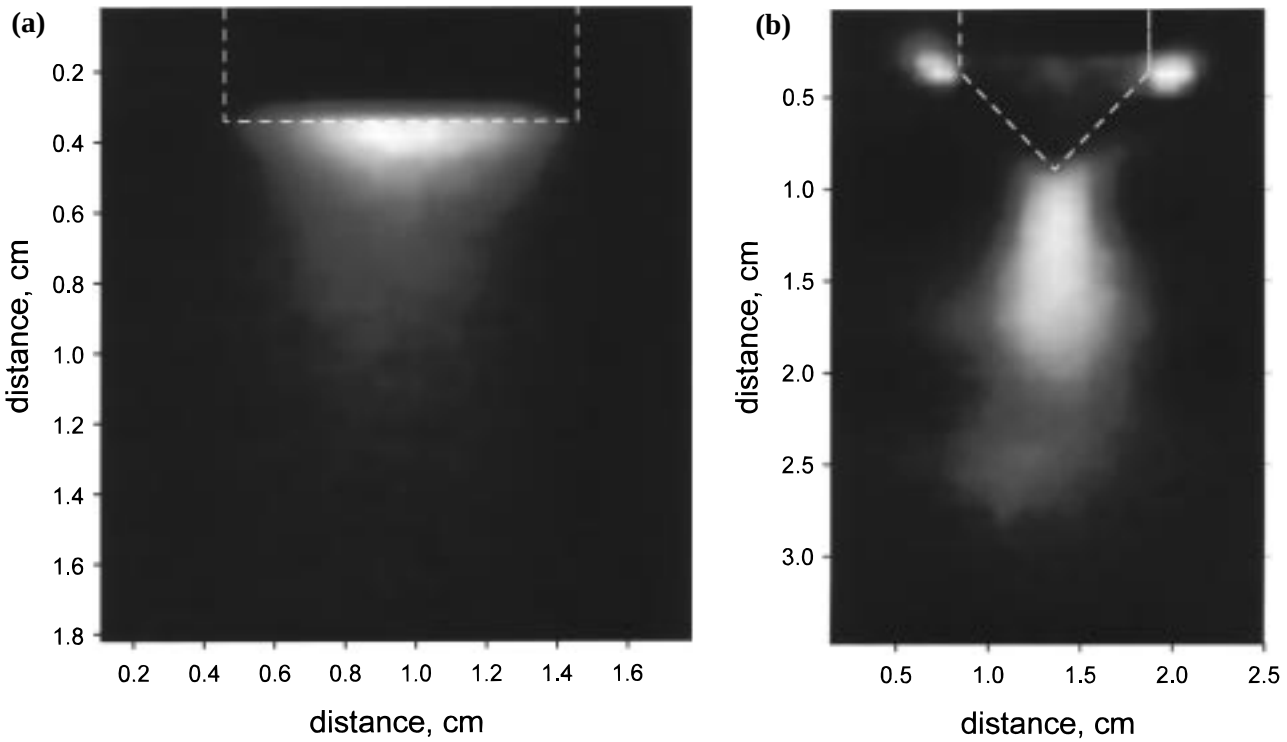

Figure 5. Images of luminol SCL activity proximal to (a) plane-ended and (b) wedge-ended 10 mm diameter cylindrical titanium sonoprobe tips: luminol concentration = 10^{-3} M; H_2O_2 concentration = 10^{-4} M; temperature = 50 °C; solution pH = 12; ultrasound power = 30 W. Tip outline indicated by white dashed lines.

provided that these were such that resonance and a standing wave pattern did not arise.

It is difficult to extract quantitative information from the images shown in Figure 5 "by eye". However the digital nature of the images permits a full analysis. Parts a and b of Figure 6 show isoluminance contour plots of spatially resolved I_{SCL} data calculated from the pixel values associated with parts a and b of Figure 5, respectively. Isoluminance contour lines were constructed using the "inverse distance squared" method of weighted average interpolation and are spaced at intervals corresponding to 10% of the maximum light intensity. It may be seen from Figure 6a that, in the case of the plane tip, maximum I_{SCL} values are located at, or very near, the transducer−solution interface and decay rapidly with distance from that interface. However, Figure 6b shows that, in the case of the wedge tip, an area of maximum I_{SCL} values occurs approximately 0.25 cm from the tip vertex and that this area is elongated coaxially with the principal axis of the transducer horn.

Images, similar to Figure 5a, of SCL emission at the plane ended sonoprobe tip were obtained over a range of transducer output power values. These images were analyzed with the

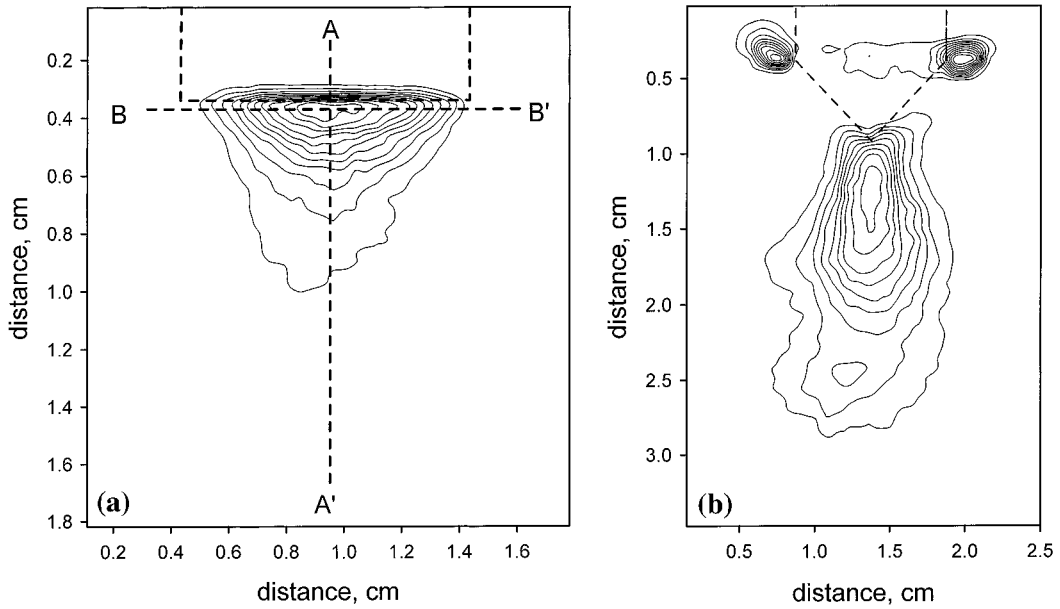

Figure 6. Isoluminance contour plots of SCL activity proximal to (a) plane-ended and (b) wedge-ended 10 mm diameter cylindrical titanium sonoprobe tips, derived from spatially resolved I_{SCL} data shown in parts a and b of Figure 5, respectively. Isoluminance contours are spaced at intervals equal to 10% of the light intensity maximum for each plot. Tip outline indicated by dashed lines.

intention of determining the extent to which the spatial distribution of SCL activity was influenced by ultrasound intensity. In all cases, I_{SCL} was found to decay exponentially with perpendicular distance (d) from the transducer surface. However, the half-length of this exponential decay was found to decrease significantly with increasing transducer output power. Figure 7a shows a semilogarithmic plot of normalized I_{SCL} values along a line coaxial with the principal axis of the ultrasound horn, as indicated by the line A−A′ in Figure 6a. The data in Figure 7a correspond to at least three half-lengths of $I_{SCL}-d$ decay. The solid lines shown in Figure 7a were constructed by least squares linear regression and exhibit gradients of 4.3 ± 0.1 cm^{-1} and 10.3 ± 0.4 cm^{-1} for transducer output powers of 5 and 70 W, respectively. Both data sets exhibit a linear correlation coefficient greater than 0.98.

By contrast, the radial distribution of I_{SCL} in the luminescent plume generated by the plane-ended sonoprobe tip was substantially independent of ultrasound output power. Figure 7b shows the distribution of normalized I_{SCL} (image pixel values) along a line normal to the principal axis of the ultrasound transducer horn, as indicated by the line B−B′ in Figure 6a, for ultrasound output powers of 5 and 70 W. It may be seen from Figure 7b that neither the shape nor the absolute width of the radial I_{SCL} distribution are changed significantly by the change in ultrasound output power. Furthermore, the diameter of the sonoluminescent plume did not change rapidly with perpendicular distance, d, from the transducer surface, i.e., the plume was not strongly divergent. In no case did the width at half-maximum value of the radially resolved I_{SCL} distribution increase by more than 10% in going from $d = 2.5$ mm to $d = 5$ mm.

Spatially Resolved I_{SCL} Values and Sonochemical Activity. In the preceding sections we have argued that I_{SCL} is proportional to the rate of sonochemical HO$^{\bullet}$ generation. However, the extent to which Figures 5 and 6 may be quantitatively interpreted as maps of sonochemical activity is not yet clear. One unknown quantity is the extent to which light scattering from cavitation bubbles[41] contributes to the SCL images. It has been stated, in the case of luminol SCL stimulated by a titanium-tipped 20 kHz ultrasound horn, that "luminescence is located on the surface of the titanium horn".[1] If this statement were literally true, the appearance of a luminescent plume in parts a and b of Figure 5 could be explained by the surface of the

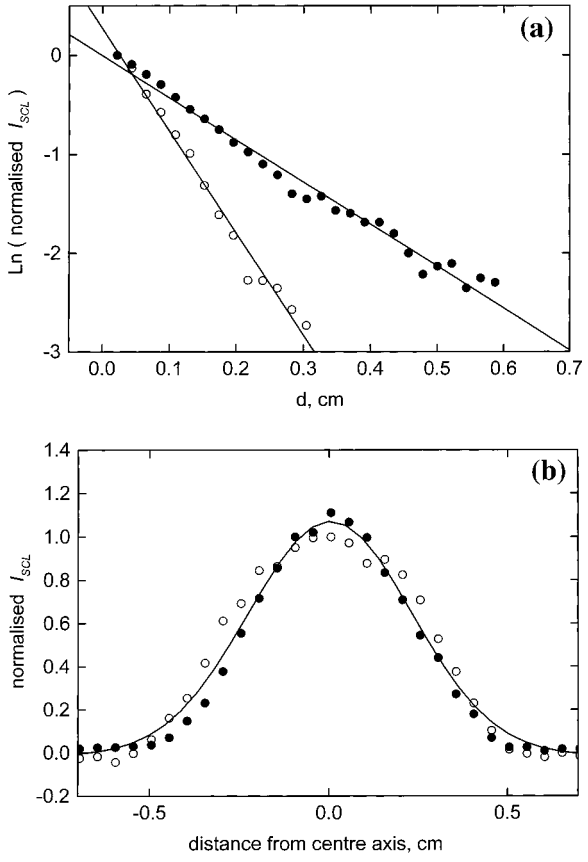

Figure 7. (a) Normalized I_{SCL} as a function of perpendicular distance d from plane-ended sonoprobe tip, i.e., along the line A−A′ shown in Figure 6a, at various ultrasound power values. (b) Normalized radial I_{SCL} distribution proximal to the plane-ended sonoprobe tip, i.e., along the line B−B′ shown in Figure 6a, at various ultrasound power values: luminol concentration = 10^{-3} M; H_2O_2 concentration = 10^{-4} M; temperature = 50 °C; pH = 12; ultrasound power = (●) 5 W and (○) 70 W.

titanium tip acting as a plane mirror, reflecting a beam of light out into solution. Light scattering by the cavitation field would then make the beam visible. That this is not the case is made evident by Figures 5b and 6b, where the direction of the principal lobe of luminescence remains coaxial with the long axis of the transducer horn (possibly due to the constructive interference of waves propagating from the tip surfaces) even though the plane surfaces of the wedge-ended sonoprobe tip lie at approximately 45° to that axis. Thus, we can conclude that, while there is probably a contribution from scattering, the light intensity distribution shown in Figures 5 and 6 derives principally from the spatial distribution of SCL activity.

The next difficulty in interpreting the images shown in Figure 5 lies in the fact that these are two-dimensional projections of a three-dimensional phenomenon. The light contributing to a single point on the image will therefore derive from a volume of luminescent solution. If the object distance is sufficiently great that light rays entering the camera lens are effectively parallel, and the absorption and scattering of light in solution are negligible, the observed light intensity will be linearly dependent on the optical path length (L) through the luminescent volume along the axis of observation. Given that the spatially resolved I_{SCL} data in Figure 5a and 6a derive from an approximately cylindrical plume of SCL activity the radially resolved I_{SCL} profiles shown in Figure 7b are expected to derive substantially from radial variation of L. Conversely, as the diameter of the luminescent plume changes very little over the first few millimeters from the transducer surface, i.e., L is approximately independent of d, the axially resolved I_{SCL} data shown in Figure 7a are be expected to correspond closely to the axial distribution of sonochemical activity. Thus, the exponential decay in I_{SCL} shown in Figure 7a reflects an exponential fall off in the rate of sonochemical $HO^{\bullet}$ generation with perpendicular distance, d, from the transducer surface.

Acoustic Attenuation in Cavitating Water. Given the preceding arguments, the axially resolved $I_{SCL}-d$ data shown in Figure 7a may be used to characterize the propagation of ultrasound travelling waves in the volume of cavitating solution proximal to the transducer surface. To facilitate the necessary analysis we will make the assumption that the axially resolved I_{SCL} values are proportional to local acoustic intensity (I, W cm^{-2}). The assumption that, microscopically, $I_{SCL} \propto I$ is not unreasonable given the linear macroscopic relationship between spatially unresolved I_{SCL} values and transducer output power shown in Figure 3. Obviously, this relationship will only apply, macroscopically or microscopically, above the cavitation threshold.

When a plane acoustic wave propagates through a homogeneous medium, the intensity of the wave decreases with distance from the radiation source due to the absorption of acoustic energy and its conversion into heat. Absorption results from viscous effects, thermal conduction, and chemical relaxation processes occurring within the medium.[42,43] The acoustic intensity, I, at some distance, d, from a source of intensity I_0 is given by

$$I = I_0 \exp(-2\alpha d) \qquad (13)$$

where α is the acoustic absorption coefficient.[42,43] For acoustic intensities below the cavitation threshold the value of α depends predictably on the mechanical and thermodynamic properties of the medium and increases with the square of the acoustic frequency, f.[42,43] For water the quantity α/f^2 has a measured value of 21×10^{-17} cm^{-1} s^2 over a wide range of frequencies,[44] implying $\alpha = 8.6 \times 10^{-8}$ cm^{-1} at 20 kHz. However, bubbles, such as those produced through cavitation, are known to be effective absorbers and scatterers of acoustic energy.[45−49] Sound absorption occurs through the damping of bubble oscillations by viscous, reradiative, and thermal conduction mechanisms,[45] and the absorption cross section of a bubble near its resonant frequency may be 1000 times its geometrical cross section.[46] For these reasons, the value of α is predicted to increase significantly in the presence of cavitation[49−51] and will depend on the number concentration and size distribution of cavitation bubbles. However, under these conditions the ultrasound wave will be subject to multiple scattering from cavitation bubbles and any experimental value of α would be more properly regarded as an "attenuation" coefficient containing both absorption and scattering contributions.

Equation 13 is immediately consistent with the exponential form of the axially resolved $I_{SCL}-d$ data shown in Figure 7a, given the assumption that $I \propto I_{SCL}$ as argued above. This being the case, the gradients of the lines shown in Figure 7a correspond to α values of 4.3 ± 0.1 cm^{-1} and 10.3 ± 0.4 cm^{-1} at I_0 values of 6.4 and 89 W cm^{-2}, respectively. The finding that, in the presence of acoustic cavitation, α values in water may increase by >8 orders of magnitude at the cavitation-producing frequency implies that, when present, cavitation is the predominant mechanism of acoustic energy absorption. It also helps to explain the observation that volumes of cavitation exert a "shielding" effect,[49] significantly reducing acoustic intensities elsewhere in a sonicated aqueous solution. The observed increase in α with I_0 suggests that either the number concentration of cavitation bubbles increases with acoustic intensity or there is an increase in their individual absorption cross sections, or both. This finding also tends to support the notion that an enhancement of acoustic absorption through cavitation may contribute to the phenomenon of "decoupling",[52] whereby the efficiency of energy transfer from the ultrasound transducer to a liquid medium decreases progressively with increasing I_0 at high I_0 values.

Conclusions

The sonogenerated chemiluminescence (SCL) of aqueous luminol is strongly influenced by pH and by the concentration of H_2O_2. In the presence of 10^{-4} M H_2O_2, the intensity of SCL is linearly proportional to ultrasound transducer output power. EDTA (10^{-4} M) reduces the background (silent) chemiluminescence of luminol/H_2O_2 solutions by $>95\%$ while minimally affecting the intensity of SCL. These findings are consistent with SCL light emission following the decomposition of a hydroperoxide adduct formed through the reaction of the luminol monoanion with sonogenerated $HO^{\bullet}$ and $O_2^{\bullet-}$. Spatially resolved light intensity information derived from digitally captured SCL video images may be analyzed to provide quantitative data on the spatial distribution of sonochemical activity in solution, provided variations in optical path length are taken into account. SCL intensity (I_{SCL}) decays exponentially with perpendicular distance (d) from a planar ultrasound transducer−solution interface and the decay half-length decreases with increasing transducer output power. Acoustic attenuation coefficients (α) in cavitating solution may be estimated noninvasively using $I_{SCL}-d$ data by assuming a linear microscopic relationship between I_{SCL} and local ultrasound intensity which reflects the observed linear macroscopic relationship between I_{SCL} and transducer output power. The α values thus obtained increase with transducer output power and may be $>10^8$ times greater than α values for homogeneous water.

In the course of the current study and the preparation of this manuscript, the authors have been made aware of promising

avenues of future work regarding the luminol SCL mechanism. Most notable of these is the use of a controlled inert gas (argon)/oxygen atmosphere. This would permit a better quantification of the role of O_2 through reactions such as reaction 11. Furthermore, elimination of N_2 would exclude the possibility of species such as NO_3^- or NO_2^-, derived from ultrasonic N_2 fixation,[53] influencing the SCL process.

Acknowledgment. The work described in this paper was funded by Maysonic Ultrasonics Ltd., U.K., and the authors thank Mr. Duncan McDonald M.D. for permission to publish. Thanks also to Dr. P. Douglas for many useful discussions.

References and Notes

(1) Pétrier, C.; Lamy, M.-F.; Francony, A.; Benahcene, A.; David, B.; Renaudin V.; Gondrexon, N. *J. Phys. Chem.* **1994**, *98*, 10514.
(2) Henglein, A.; Ulrich, R.; Lilie, J. *J. Am. Chem. Soc.* **1989**, *111*, 1974.
(3) Henglein, A.; Herburger, D.; Gutiérrez, M. *J. Phys. Chem.* **1992**, *96*, 1126.
(4) Gonze, E.; Gonthier, Y.; Boldo, P.; Bernis, A. *Chem. Eng. Sci.* **1998**, *53*, 523.
(5) Renaudin, V.; Gondrexon, N.; Boldo, P.; Pétrier, C.; Bernis, A.; Gonthier, Y. *Ultrason. Sonochem.* **1994**, *1*, S81.
(6) Merényi, G.; Lind, J. S. *J. Am. Chem. Soc.* **1980**, *102*, 5830.
(7) Lind, J. S.; Merényi, G.; Eriksen, T. E. *J. Am. Chem. Soc.* **1983**, *105*, 7655.
(8) Vitt, E. J.; Johnson, D. C. *J. Electrochem. Soc.* **1991**, *138*, 1637.
(9) Sakura, S. *Anal. Chim. Acta* **1992**, *262*, 49.
(10) Mason, T. J. *Sonochemistry—The Uses of Ultrasound in Chemistry*; The Royal Society of Chemistry: Cambridge, 1991; Chapter 2, pp 18−21.
(11) Entezari, M. H.; Kruus, P. *Ultrason. Sonochem.* **1996**, *3*, 19.
(12) Bottu, G. *J. Biolumin. Chemilumin.* **1991**, *6*, 147.
(13) Klopf, L. L.; Niemann, T. A. *Anal. Chem.* **1983**, *55*, 1080.
(14) Seitz, W. R.; Hercules, D. M. In *Chemiluminescence and Bioluminescence*; Cormier, M. J., Hercules, D. M., Lee, L., Eds.; Plenum Press: New York, 1973; pp 427−229.
(15) Krika, L. J.; Xiaoying, J.; Thorpe, G. H. G.; Edwards, B. E.; Voyta, J.; Bronstein, I. *J. Immunoassay* **1996**, *17*, 61.
(16) Suslick, K. S. *Science* **1990**, *247*, 1439.
(17) Buxton, G. V.; Sellers, R. M. *Radiat. Phys. Chem.* **1987**, *29*, 137.
(18) Kochany, J.; Lipczynskakochany, E. *Chemosphere* **1992**, *25*, 1769.
(19) Buxton, G. V.; Elliot, A. J. *Radiat. Phys. Chem.* **1986**, *27*, 241.
(20) Buxton, G. V.; Greenstock, C. L.; Helman, W. P.; Ross, A. B. *J. Phys. Chem. Ref. Data* **1988**, *17*, 513.
(21) Suslick, K. S. *Sci. Am.* **1989**, *260*, 80.
(22) Henglein, A. *Ultrasonics* **1987**, *25*, 6.
(23) Verall, R. E.; Sehgal, C. M. in *Ultrasound—Its Chemical, Physical and Biological Effects*; Suslick, K. S., Ed.; VCH Publishers: New York, 1988; Chapter 6, p 227.
(24) Makino, K.; Mossba, M. M.; Riesz, P. *J. Am. Chem. Soc.* **1982**, *104*, 3537.
(25) Fischer, C.-H.; Hart, E. J.; Henglein, A. *J. Phys. Chem.* **1986**, *90*, 1954.
(26) Hart, E. J.; Henglein, A. *J. Phys. Chem.* **1987**, *91*, 3654.
(27) Makino, K.; Mossoba, M. M.; Riesz, P. *J. Phys. Chem.* **1983**, *87*, 1369.
(28) Suslick, K. S.; Grinstaff, M. W. *J. Am. Chem. Soc.* **1990**, *112*, 7807.
(29) Hart, E. J.; Henglein, A. *J. Phys. Chem.* **1985**, *89*, 4342.
(30) Lippet, B.; McCord, J. M.; Fridovich, I. *J. Biol. Chem.* **1972**, *247*, 4688.
(31) Weissler, A. *J. Am. Chem. Soc.* **1959**, *81*, 1077.
(32) Hart, E. J.; Henglein, A. *J. Phys. Chem.* **1986**, *90*, 1954.
(33) Hart, E. J.; Henglein, A. *J. Phys. Chem.* **1987**, *91*, 3654.
(34) Rabani, J.; Neilsen, S. O. *J. Phys. Chem.* **1969**, *73*, 3736.
(35) Baxendale, J. H. *Radiat. Res. Suppl.* **1964**, *4*, 114.
(36) Merényi, G.; Lind, J. S.; Eriksen, T. E. *J. Phys. Chem.* **1984**, *88*, 2320.
(37) Erdey, L.; Buzás I.; Vigh, K. *Talanta* **1966**, *13*, 463.
(38) Baxendale, J. H. *J. Chem. Soc., Faraday Trans. 1* **1973**, *69*, 1665.
(39) Eriksen, T. E.; Lind, J.; Merényi, G. *J. Chem. Soc., Faraday Trans. 1* **1983**, *79*, 1493.
(40) Ross, F., Ross, A. B., Eds. *Natl. Stand. Ref. Data Ser., Natl. Bur. Stand.* **1977**, 59.
(41) Barber, B. P.; Putterman, S. J. *Phys. Rev. Lett.* **1992**, *69*, 3839.
(42) Mason, T. J. *Sonochemistry—The Uses of Ultrasound in Chemistry*; The Royal Society of Chemistry: Cambridge, 1991; p 12.
(43) Mason, T. J.; Lorimer, J. P. *Sonochemistry—Theory, Applications and Uses of Ultrasound in Chemistry*; Ellis Horwood: Chichester, 1989; Chapter 2, p 25.
(44) Fox, F. E.; Rock, G. D. *J. Acoust. Soc. Am.* **1941**, *12*, 505.
(45) Apfel, R. E. In *Methods of Experimental Physics: Ultrasonics*; Edmonds, P. D., Ed.; Academic Press: New York, 1981; Vol. 19, Chapter 7, p 355.
(46) Pace, N. G.; Cowley, A.; Campbell, A. M. *J. Acoust. Soc. Am.* **1997**, *102*, 1474.
(47) Suiter, H. R. *J. Acoust. Soc. Am.* **1992**, *91*, 1383.
(48) Hilgenfeldt, S.; Lohse, D.; Zomack, M. *Eur. Phys. J. B*, **1998**, *4*, 247.
(49) Leighton, T. G. *Ultrason. Sonochem.* **1995**, *2*, S123.
(50) Mason, T. J.; *Sonochemistry—The Uses of Ultrasound in Chemistry*; The Royal Society of Chemistry: Cambridge, 1991; p 14.
(51) Watkin, N. A.; terHaar, G. R.; Rivens, I. *Ultrasound Med. Biol.* **1996**, *22*, 483.
(52) Mason, T. J. *Practical Sonochemistry—A User's Guide to Applications in Chemistry and Chemical Engineering*; Ellis Horwood: London, 1991; Chapter 1, p 24.
(53) Virtanen, N.; Ellfolk, N. *J. Am. Chem. Soc.* **1950**, *72*, 1046.